Journal of Coastal Conservation 2: 23-32, 1996

Assessing wetland changes in the Venice lagoon by means of satellite remote sensing data

Brivio, P.A.* **& Zilioli, E.**

Remote Sensing Dept., Istituto di Recerca sul Rischio Sismico - CNR-IRRS, Via Ampère 56, I-20131 Milano, Italy;
**Fax +39 2 70643660; E-mail brivio@tel-irrs.mi.cnr.it*

Abstract. Not only does lagoon ecology represent a transitional zone between the sea and the continent but it also expresses the equilibrium belt between erosion and sedimentation processes. Within the framework of a coastal management scheme, a precise and timely mapping of morphological changes in this environment is important. This paper illustrates the possible contribution of multi-temporal satellite observations in the monitoring of the erosion/sedimentation processes of coastal zones, where landscape features are subjected to highly morphodynamical modifications. In particular, an improved mapping accuracy was obtained by the successive application of the Maximum Likelihood (MLH) classifier and the Linear Mixture Model (LMM) techniques to the satellite image classification procedure. In fact, by estimating the amount of shallow water and wetland within each satellite pixel, the LMM technique allows for an accurate mapping of the transitional zones in the lagoon environment, thus permitting an optimal separation between land and water. The study concerns the Venice lagoon (Italy) which has been sinking slowly since the beginning of this century. This has led to widespread loss of wetlands. In order to monitor the development of the land cover, four Landsat Thematic Mapper scenes were examined, during the period 1984 to 1993. The results obtained proved that the digital analysis method of multitemporal satellite imagery, applied over a selected test area, enables the evolution of an estuarine environment landscape, with its different sequences of erosion and periods of accretion, to be monitored. The significant influence of tidal stages is discussed in the data analysis.

Keywords: Image classification; Landsat; Linear Mixture Model; Maximum likelihood; Morphodynamics; Subsidence.

Introduction

Most of the world's wetlands are deteriorating and decreasing in area. This results in serious problems in the management of natural coastal resources, especially where anthropic presence is widespread and man's influence strong. Due to the impact of man's presence since the Middle Ages, the Venice lagoon (Italy) is one of the most delicate examples of these types of ecosystems in the world. In general, gains and losses are a part of estuarine sedimentation processes and there is no standard wetland increase in estuarine processes. In the case of the Venice lagoon, historical observations have recorded a slow sinking, with the highest peaks in the 1950s and 1960s, the most precise and reliable documentation dates back to the beginning of this century.

In the past most of the problems pertaining to the equilibrium of the ecosystem seemed chiefly to be ascribed to land subsidence (caused not only by sediments trapped in reservoirs and groundwater withdrawals, but also by eustasy (Gatto & Carbognin 1981). Currently, intertidal erosion mainly results from the combined actions of different hydrodynamical processes, such as man-induced morphological changes, and consequently increased currents, not to mention the effects of tidal flooding and periodic 'high-waters'; the latter triggered off by a coincidence of particular atmospheric and astronomical conditions that occur in the Adriatic sea (Santangelo et al. 1982; Cavazzoni & Crosera 1987; Carbognin et al. 1995). As outlined in previous studies, where maps and historical documentation have been compared in detail, this results in a general and extensive loss of wetlands. The sinking of the lagoon was first ascertained by comparing early 16th- century documentation with the large-scale hydrographic charts compiled in 1930 (Cisotto 1968). Further studies on this subject were based on more recent documentation, such as the cartogram drawn in 1810 by Denaix (Betetto 1973) and the hydrographic maps at 1:5000 dating back to 1930 and 1971 (Rusconi 1987). Finally, this analysis was extended to the present, by means of cartograms drawn in 1987 and various series of recent aerial photographs (Anon. 1989, 1992). With regard to the last century, different surveys have demonstrated that 40% of the *barene* - the local name for wetlands - was lost in the 40-yr period from 1930 to 1970; further erosion has also been ascertained over the last 20 years, as a continuation of the negative trend observed earlier. It can therefore be said that during the present century about 70 % of the wetlands, that account for the entire Venice lagoon, have been lost; decreasing from an extension of about 130 to 40 km^2 (Adami et al. 1992). Fig. 1 shows the changes of the most important land-cover units since the beginning of the century. A linear extrapolation of the trend observed, projected forwards over future decades, pre-

dicts a total loss of the wetlands by the year 2050.

The loss of wetlands causes serious damage to the whole ecosystem. In fact, intertidal wetlands and shallow zones are major areas of biological productivity where the nutrient load, which is responsible for the hypertrophic state of the lagoon, can be assimilated by plant communities/vegetation and subsequently fed to superior species of the biological chain. In the Venice lagoon the total amount of nutrients is 1100 tons/yr of nitrogen and 1500 tons/yr of phosphorus; exceeding the assimilation capability of the ecosystem by a factor of 3 (Anon. 1992).

Moreover, the long-term increase in 'greenhouse' gases in the atmosphere has led to a warming of the Earth's surface (Anon. 1987; Wigley & Raper 1993). Although the climate change is still quite a controversial issue among many scientists, different models estimated potential temperature increases of between 1.5 and 4.5 °C (Clark & Primus 1990; Nilsson 1992). This may produce a significant increase in the global sea level (numerous predictions of low-end and high-end rise have been predicted for the year 2100) from 0.6 to 2.3m (Thomas 1986) or from 0.03 to 1.24m (Wigley & Raper 1993). Any of the aforementioned predictions could have a strong impact on coastal wetland regions which are close to the present mean sea level.

It thus becomes very important to develop a methodology to monitor the wetland changes underway. In order to predict which processes will dominate what locations in the future, this can even be conducted on a small spatial scale and at a suitable temporal resolution. This valuable information could be provided by the space observations of remote sensing satellites. Although with different objectives, early remote sensing was applied to coastal morphology in the 1970s, either in different environments (e.g. Verger & Demathieu 1973), or specifically in the Venice lagoon (Alberotanza & Lechi 1978). But, as demonstrated by several studies (e.g. Gross et al. 1987; Haddad & Ekberg 1989; Jensen et al. 1993a), it was only in 1982, when high resolution sensors such as the Landsat Thematic Mapper (whose technical characteristics are reported in Table 1) began operating that remote sensing was able to offer a suitable instrument to map lagoon landscape units.

Due to the fact that geomorphological forms frequently display a certain heterogeneity and a complex dendritic structure, lagoon landscape patterns often present a difficult environment to map. Since we were interested in accurately mapping the transition zones between the shallow water and the wetlands, the main problem to be considered was to estimate the amount of each component within each pixel (Adams et al. 1986). The approach adopted here for an accurate mapping of wetlands, was based on the sequential application of the Maximum Likelihood Classifier (MLH) and the Linear Mixture Model (LMM) techniques used in the satellite image classification procedure. As shown by previous works, linear mixture modeling proved to be the most appropriate technique for estimating sub-pixel proportions, by assuming a realistic, physically based model of sub-pixel spectral mixing (e.g. Hurcom et al. 1993). Accurate land-cover maps were derived from a combined MLH and LMM analysis of four Landsat Thematic Mapper passages conducted over an entire decade from 1984. A comparative analysis of land-cover temporal changes, dealing with wetland decrease/increase processes, is also outlined and discussed.

Study area and data used

Previous papers on the subject showed evidence of a sparse loss of wetlands throughout the whole Venice lagoon, while the largest accretion proved to be predominantely in the central-southern part of the lagoon (Rusconi 1987; Anon. 1989). However, since the objective of the research was strictly dependent on a reliable validity test of the data derived from the satellite observations (requiring a precise calibration reference)

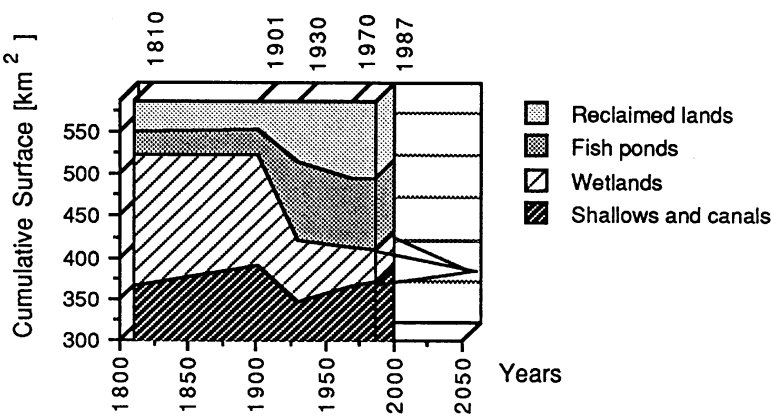

Fig. 1. Development since 1810 of the main landscape units in the Venice lagoon. Complete loss of wetland areas could be expected by 2050 (adapted from Adami et al. 1992).

Table 1. Spatial and spectral characteristics of Landsat Thematic Mapper. Orbital altitude 705 km, coverage frequency 16 days, swath width 180 km (Markham & Barker 1985).

Sensor	Spectral Interval (μm)	Band	Ground Resolution (m)
TM-1	0.452 - 0.518	Blue-Green	30
TM-2	0.528 - 0.609	Green-Yellow	30
TM-3	0.626 - 0.693	Red	30
TM-4	0.776 - 0.904	Near Infrared	30
TM-5	1.567 - 1.784	SW-Infrared 1	30
TM-7	2.097 - 2.349	SW-Infrared 2	30
TM-6	10.45 - 12.42	Thermal Infrared	120

the choice of the study area depended mainly on the availability of any information that was as simultaneous as possible with respect to the satellite overpass. This opportunity was provided by the existence of a set of colour aerial photographs taken over some spots in the northern part of the lagoon, simultaneously with the 1987 satellite image. Moreover, as shown by the data in Table 2, this area showed both positive and negative change gradients in the land cover units, that are sufficiently easy to detect in the ten-year period considered.

The study area corresponds to a 266 × 141 pixel window (about 34 km^2) in the satellite images (Fig. 2); this accounts for 6% of the total lagoon surface which, according to the borderline defined in 1900 by the Magistrato alle Acque di Venezia, extends over an area of 586 km^2. Roughly speaking, the area chosen is situated in the northern part of the Island of Burano, and includes several salt marshes such as the Palude di Cona, the Palude della Rosa, the Palude della Centrega and the Palude del Tralo.

The bathymetry of the Venice lagoon is characterized by very low depths ranging between – 0.5 m and –2.0m, excluding canals; generally speaking, tidal differences are relatively low, accounting for a few decimeters, with a maximum of about 1m within the syzygial tides. Tidal stage is an important factor in studies of this nature, since even a small increase in the mean sea level may influence the water sheet distribution throughout the whole lagoon and consequently lead to possible errors in the comparative analysis of temporal data sets. Furthermore, this influence varies according to tidal wave propagation in the lagoon.

Since for this study multi-temporal analysis of satellite data is necessary, ideally constant tidal stage values are required but this severely reduces the amount of satellite imagery available. To overcome this problem and in order to include the necessary corrections which, on the contrary, were not considered in this study, these results should be deduced from topographical information, such as intertidal microtopography.

Moreover, in order to avoid excessive presence of algal blooms, which peak in early spring and fall months, satellite scenes were selected outside these times. This could affect both the quality of the results and the accuracy of the classification but could also lead to land-cover misidentification. Bearing these factors in mind, a set of four Landsat-TM images, taken at three-yearly intervals during the period 1984-1993 (Table 3) were selected. Table 3 also shows the mean tidal stage values at Lio Piccolo (located within the same study area) expressed in centimetres above mean sea level. These data were calculated by differential analysis according to the model indicated by Goldmann et al. (1975). This shows a delay time of 73minutes and a 0.83 gain coefficient with respect to the tidal stage at the nearby 'Diga Sud Lido' marigraphic station which is located on a dam between the two major sand banks that separate it from the open sea.

The 1984 and 1993 Landsat images, at the extremes of the ten year interval, show an identical tidal stage, thus allowing for direct and reliable comparison of the results. The 1987 tide level was slightly lower, inferring an overestimation of wetland extension with respect to both 1984 and 1993. On the contrary, tidal conditions on 19 July 1990 (when the image was taken) were quite different, showing a 16 cm higher tidal stage, which was

Table 2. Wetland changes according to a comparison of hydrographic maps published in 1930 and 1970. Each section corresponds to about 5 km^2 (after Rusconi 1987).

Section #	Name	Wetland extent (km^2)		Difference (km^2)
		1930	1970	
26	Palude di Cona	1.549	1.259	– 0.290
27	S. Ariano	1.448	1.107	–0.341
28	S. Cristina	1.568	1.400	–0.168
33	Lio Piccolo	0.242	0.183	–0.059
38	Burano	1.137	0.978	–0.159
39	Centrega	1.355	1.553	0.198
40	S. Felice	1.020	1.115	0.095

Table 3. Satellite and aerial remote sensing data used in the study together with the mean tidal stage values at Lio Piccolo measured in cm above mean sea level (a.m.s.l.)

Survey Type	Date	G.M.T.	Tidal Stage
Landsat TM	03-08-1984	09.40	7.83 cm
Landsat TM	08-05-1987	09.40	4.70 cm
Landsat TM	19-07-1990	09.40	23.50 cm
Landsat TM	24-05-1993	09.40	7.88 cm
Aerial Photo	08-05-1987	09.42	4.70 cm

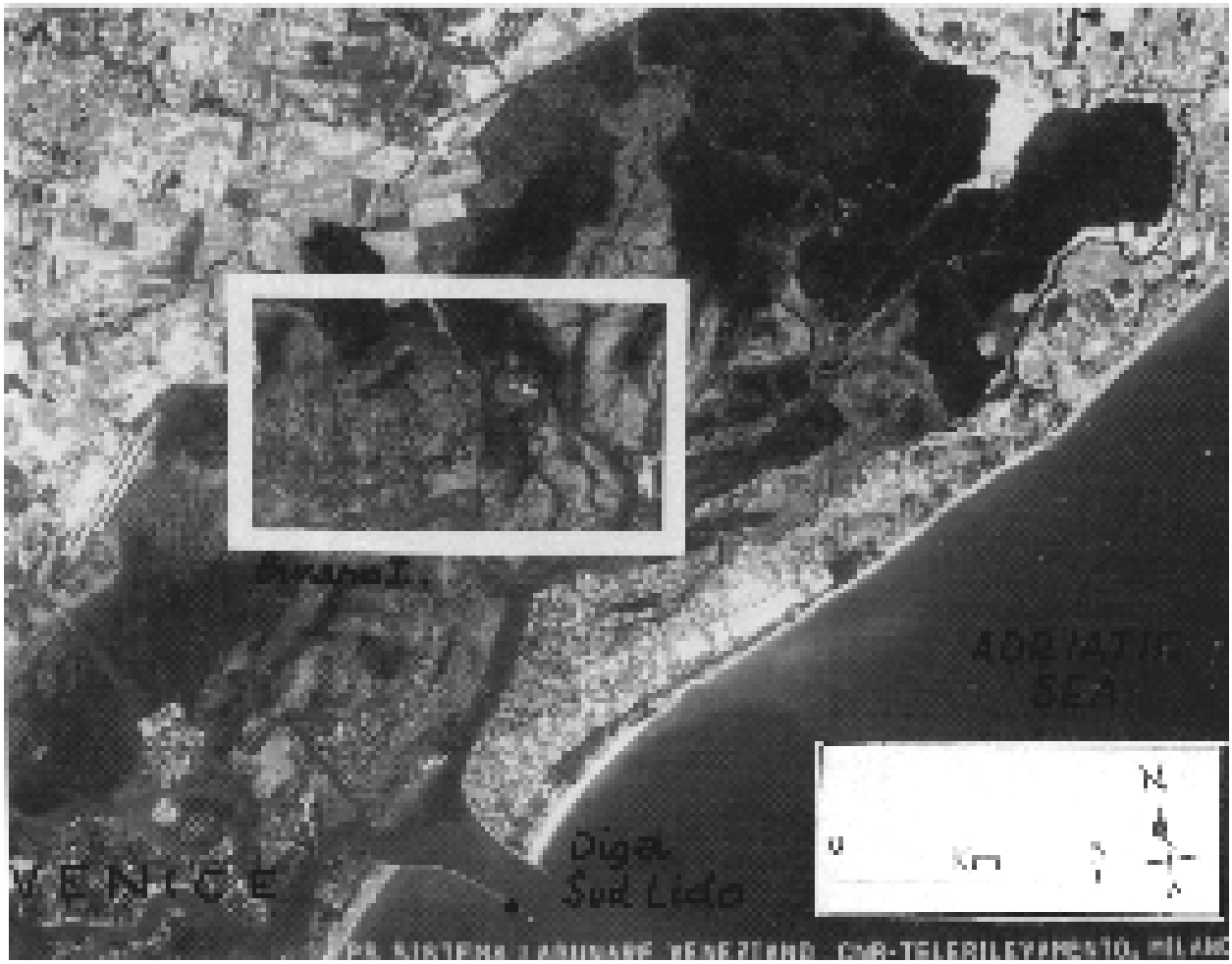

Fig. 2. North-eastern part of Venice lagoon. Landsat Thematic Mapper multispectral image (24 May 1993; RGB: TM4,TM1,TM5) elucidates the complex environment of the transitional zones between the mainland and the open sea. The rectangle outlines the study area.

sufficient to make these data unusable and were excluded from further analysis. Owing to the fact that, in order to obtain a more precise evaluation, data should be corrected from the tide influence by means of a suitable DEM (Digital Elevation Model) which accurately describes the topography and the bathymetry of the area (Jensen et al. 1993b).

Colour aerial photographs (at scale 1: 20000) taken on 8 May 1987 at the same time as the satellite overpass, were also available for the selected site. These photographs were taken during the routine aerial surveys, planned by the Regione del Veneto, to update official cartography. This was really an uncommonly lucky coincidence and a great opportunity which is usually extremely difficult to accomplish even by means of finalized surveys and *ad hoc* programmes. These high resolution images were used as an independent reference to test and validate the maps obtained from the satellite classification procedure.

A ground survey was conducted in order to recognize the main land-cover units: water, submerged algae, bare land and wetland. More precisely, the bare land category consists of tidal mud flats (i.e. unconsolidated wet sediments) and the wetland category is generally occupied by halophytic vegetation including *Limonium venetum*, *Puccinellia palustris* and *Salicornia herbacea*.

A spectro-radiometer, operating within the 0.4-1.0 μm range, was also used to take a series of radiometric measurements in the lagoon. Although the instruments' spectral range does not include the mid infrared bands (Landsat TM5 and TM7), a consistent contrast between the two main classes, water and wetland, were found in the infrared wavelengths, as shown in Fig. 3.

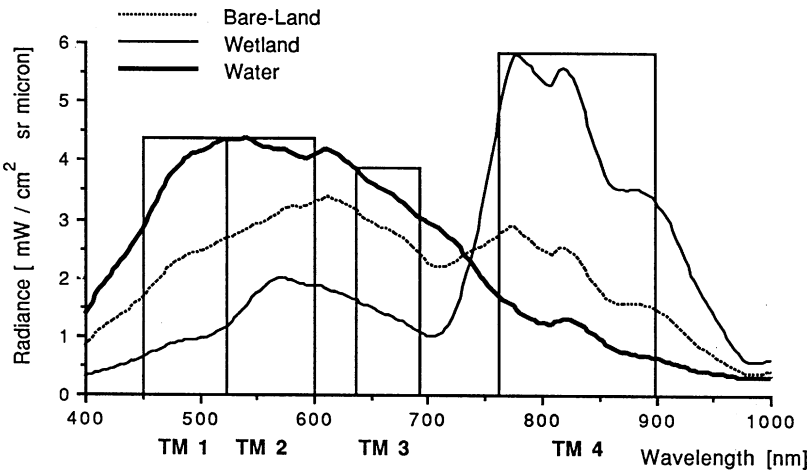

Fig. 3. Examples of spectral signatures for the three main land-cover classes in the Venice lagoon; these are derived from radiance data collected during a ground reconnaissance survey conducted on 14 July 1993.

Satellite image classification procedure

Since the advent of remote sensing satellite for Earth resources exploration, digital classification methods of multispectral satellite imagery have been gaining in importance for automatic land-cover mapping. Statistical classification techniques generally make use of probability functions associated with pattern classes. These are referred to as parametric if the data distribution form in the *N*-dimensional feature space is assumed to be known in advance and non-parametric if only certain parameters need to be estimated from the training patterns. The classification process may also be supervised, when training samples aimed at learning the spectral characteristics of the informational classes are used, or unsupervised when, for a number of reasons, the supply of training samples is not available or is severely limited (Swain & Davis 1978; Richards 1986).

Maximum-likelihood technique

The most widely accepted pixel assignment supervised methodology for land-cover mapping applications is the maximum-likelihood (MLH) technique (Hardin 1994). The supervised MLH classifier is a parametric technique which assumes that each of the categories examined has a multivariate normal distribution in the space of the *N* spectral bands of the satellite sensors. The parameters that typically summarize the statistical characteristics of the training data, i.e. known pixels assumed as a representative pattern of each land-cover class, include mean vectors **M**, variance-covariance matrices **C** and prior probabilities p_k for each class k (k = 1, ..., K).

The maximum-likelihood decision rule requires the assignment of an unknown pixel, with a measurement vector **x** associated to class k if

$$p(\mathbf{x} \mid k) * (p_k) \geq p(\mathbf{x} \mid i) * (p_i) \text{ for all } i \neq k \qquad (1)$$

where $p(\mathbf{x} \mid k)$ is the class conditional probability (Swain & Davis 1978). For a multivariate normal distribution, the discriminant function D to be minimized for each pixel, according to MLH approach, is given by the following formula:

$$D_k(\mathbf{x}) = \ln(p_k) - 1/2 \ln|\mathbf{C}| - 1/2 (\mathbf{x} - \mathbf{M})^T \mathbf{C}^{-1} (\mathbf{x} - \mathbf{M}) \qquad (2)$$

where **x** is the pixel measurement vector, **M** is the *N*-dimensional mean vector of class k under examination, **C** is the $N \times N$ variance-covariance matrix of class k, and p_k is the prior probability of class k.

The final result of the MLH is a single image, or a map, where a label identifying the category is associated to each pixel.

Linear mixture modeling

Conventional multispectral satellite data classification techniques, such as the maximum-likelihood technique described above, are well suited to dealing with 'pure' pixels since they give one category per pixel: these pure signals are termed endmember spectra (Adams et al. 1986). In the case of a complex landscape pattern such as the lagoon environment, it is far more likely that an individual pixel will contain a mixture of different land-cover categories. Consequently, linear mixture modeling (LMM) was selected as a more appropriate technique for estimating the proportion of each component within each pixel (Shimabukuro & Smith 1991; Holben & Shimabukuro 1993).

Since the response of each pixel, in any spectral band n, includes the influence exercised by two or more categories k, the resulting at-satellite radiance value L_n can be seen as

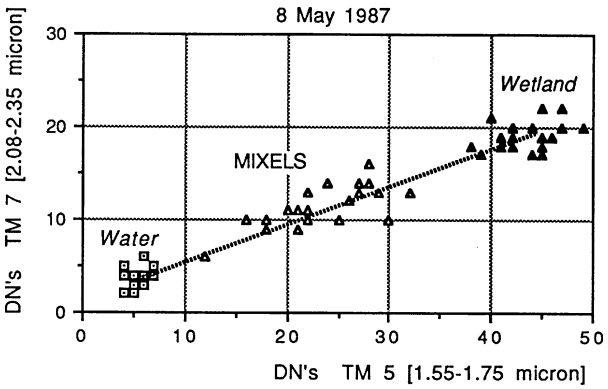

Fig. 4. Spectral distribution of samples from pure member, water and wetland, and mixed pixels (mixels) in the spectral space of the Landsat Thematic Mapper infrared bands TM7 and TM5. Radiance measurements are expressed in digital numbers (DN).

a linear combination of the responses $r_{k,n}$ of each component assumed to be in the mixed target (Fig. 4).
The basic mixture model can be formulated as:

$$L_n = \sum_{k=1}^{k} \left(r_{k,n} \cdot x_k \right) + e_n \qquad (3)$$

L_n = at-satellite radiance value in the spectral band n; $r_{k,n}$ = expected spectral response of component k in the spectral band n; x_k = proportion for a pixel of component k; e_n = error term for spectral band n.
A linear constraint is added, the sum of the proportions must be one ($\Sigma\, x_k = 1$) for any pixel and the proportion values must be non-negative ($0 \leq x_k$). The least-square method applied by means of the generalized inverse matrix (Terayama et al. 1992) is used to estimate the proportions x_k of the components inside the pixel by minimizing the sum of the squares of the errors:

$$E = \sum_{n=1}^{N} \left(e_n \right)^2 \rightarrow \min \qquad (4)$$

The final result of the unmixing process is a set of fraction maps, one for each of the selected categories, with the pixel value scaled from 0 to 100 %, representing the proportion of land occupation in that category.

Analysis of the results

The three reflective infrared bands of Landsat-TM, i.e. TM4, TM5 and TM7, which guaranteed a sufficient contrast between water and wetland classes, were used in both MLH and LMM classification procedures. The identification of 'pure' pixels corresponding to both water and wetlands according to a visible band spectral response would suffer too much from the quality of the shallow water in the lagoon (Zilioli et al. 1994). Moreover, the LMM method was developed for two components or main categories, water and wetland, assumed to be present inside the mixed target. The proportionate area in the pixel is evaluated on the basis of the orthogonal projection of the mixed pixel spectral components onto the line joining the mean values of the pure members (Fig. 4).

Spatial pattern

For each satellite scene, a digital classification, using a supervised maximum-likelihood technique, was performed. A set of training areas, representing the four land-cover classes (water, submerged algae, bare land and wetland), were identified on TM imagery with the support of the ground reconnaissance survey. To help ensure consistency between image dates, the same training areas were used; the selection of near and mid infrared wavelengths also minimize the atmospheric effects. Spectral statistics were then calculated for each of the three infrared TM bands.

The results obtained from the classification process are shown in Table 4, where each category of land-cover extension is expressed both as an absolute number of pixels and as a percent of the total surface. Subsequently, these land cover classes were aggregated to produce two broad categories, water (water mass and submerged algae) and wetlands (wetland and bare land). Table 4 also shows the mean tidal stage values in centimetres above mean sea level at Lio Piccolo.

Finally, the land-cover category indicated in Table 4 as 'unclassified/mixed', refers to those pixels which, having probabilities for all classes lower than a threshold value, were rejected by the decision process (Richards 1986). In this experiment, patterns having probabilities lower than 5 % were interpreted as mixed targets and analyzed according to the following procedure.

The linear mixture modeling (LMM) approach was then applied in order to obtain a sub-pixel estimation of the spatial extent of wetlands and water for mixed targets rejected by the MLH classifier. Training samples, used in the MLH classification, allowed us to define endmember spectra, in the three infrared TM bands of the two informational classes water and wetland (Fig. 4). For each of the Landsat scenes examined, the final result consists of proportion images where, for each pixel, the percentage of area belonging to the category in question is indicated. Figures indicating land-cover extension obtained by the application of LMM technique are shown in Table 5, where pixel numbers represent the accumulated sum of partial pixels.

Table 4. Results of maximum likelihood (MLH) classification for the three satellite scenes using infrared bands TM4, TM5 and TM7. Total number of pixels is 37 506.

Date	03 August 84		08 May 87		24 May 93	
Mean Tidal Stage (cm)	7.83		4.70		7.88	
Land-Cover	# Pixels	[%]	# Pixels	[%]	# Pixels	[%]
Wetland	6793	18.11	5949	15.86	6891	18.37
Bare Land	4172	11.12	1900	5.07	3058	8.15
Total land	10965	29.23	7849	20.93	9949	26.52
Water	10316	27.50	13161	35.09	19890	53.03
Submerged Algae	4214	11.24	6706	17.88	1410	3.76
Total water	14530	38.74	19867	52.97	21300	56.79
Unclassified / mixed	12011	32.03	9790	26.10	6257	16.68

Validation of satellite image analysis

In order to test the performance of the MLH classification method, an accurate visual inspection of satellite derived maps was conducted by an expert. Testing was conducted on a 409 pixels population selected in the image using a stratified random sampling technique (Fitzpatrick-Lins 1981).

Table 6 presents the results of the accuracy assessment for the MLH classification of the 8 May 1987 Landsat image. Descriptive statistics calculated from contingency tables include 'producer's accuracy' which is a measure of omission errors, 'user's accuracy' which accounts for commission errors and overall accuracy, i.e. total percent correct (Congalton 1991). Several misclassifications occurred at the sub-class level, especially for submerged algae and bare land categories. Following the aggregation of the different sub-classes into two relevant land-covers, water and wetland, final overall accuracy was 87.53%.

For the three satellite passages overall accuracy figures were in the 87-92% range.

Validation of the LMM approach was achieved by comparing the results with the higher resolution data of available aerial photographs taken simultaneously with the 1987 Landsat imagery. Colour aerial photographs were digitized at a 5 meter ground resolution and displayed on a computer screen. An accurate mapping of 10 different site-samples separately in the aerial photographs and in the satellite imagery was conducted by recognizing, pixel by pixel, the two main land-cover categories: water and wetland. The comparison between water and wetlands occupation, as deduced from the LMM approach and from direct photo-interpretation of aerial data, indicates the accuracy of the method. The results of this test, presented in Table 7, give a total underestimation of 10 ha for the water surface extension in 7 sites and a total overestimation of 3.7 ha in the remaining 3 samples. Thus the satellite derived map indicated an overall overestimation of 5.8 % in wetland land-cover.

Land-cover temporal variation

Results from the final mapping obtained by the successive application of the MLH classifier and the LMM technique are summarized in the Table 8, where land occupation by two categories, wetland and water, is shown as a number of pixels, square kilometres and percentage of the study area.

During the period 1984 to 1993, a slight general increase of the extent of the water surface was observed, showing an increase of from 19.8 km^2 to 20.7 km^2, with a consequent reduction of the wetland surface. The rate of wetland loss of 0.102 km^2/yr, observed over the entire period between 1984-1993 within the study area, differs significantly from the average value of 0.701 km^2/yr observed throughout the whole lagoon in the period between 1930-1987 (Adami et al. 1992).

Table 5. Results of Linear mixture model (LMM) analysis for the three satellite scenes, using infrared bands TM4, TM5 and TM7.

Date	03 August 1984		08 May 1987		24 May 1993	
Mean tidal stage (cm)	7.83		4.70		7.88	
Land-cover	# Pixels	(%)	# Pixels	(%)	# Pixels	(%)
Mixed pixels	12011	100.00	9790	100.00	6257	100.00
Water	7469	62.18	5180	52.91	4533	72.45
Wetland	4542	37.82	4610	47.09	1724	27.55

Table 6. Contingency table for maximum likelihood (MLH) classification of 8 May 1987 Landsat image. Test pixels 409.

	Reference data					Accuracy	
	Water	Algae	Wetland	Bare land	Total	Producer's	User's
Water	123	8	6	8	145	123/135 = 91%	123/145 = 85 %
Algae	4	51	19	-	74	51/69 = 74%	51/74 = 69 %
Wetland	2	6	119	10	137	119/150 = 79%	119/137 = 87 %
Bare Land	6	4	6	37	53	37/55 = 67%	37/53 = 70 %
	135	69	150	55	409	Overall Accuracy : 330/409 = 81 %	

Table 7. Comparison between surface water extension in 10 site-samples as derived from LMM analysis of 8 May 1987 Landsat image and from visual interpretation of colour aerial photographs.

Site-sample #	Water extent (ha) Satellite data	Aerial data	Difference (ha)
01	13.84	14.30	– 0.46
02	15.01	18.98	–3.97
03	10.54	13.03	–2.49
04	8.90	7.24	+ 1.66
05	9.89	8.37	+1.52
06	13.07	12.55	+0.52
07	13.07	13.66	–0.59
08	3.40	3.97	–0.57
09	4.18	4.75	–0.57
10	9.65	11.02	–1.37
Total	101.56	107.86	–6.30 [a]

[a] This difference corresponds to an overall underestimation of 5.84% in water extension.

The comparative analysis of changes in the land cover extent was proved by differently combining the following three time periods: 1984-1987, 1987-1993, and 1984-1993 and always considering the influence of each relative tidal variation.

The temporal variations in wetland surface extension are summarized in Table 9, where, together with the changes expressed as absolute and percentage values, a rate of change is also indicated as km^2 per year.

Some interesting observations, suggesting different trends in temporal changes, can be seen in Table 9:

- the first period, from 1984 to 1987, had an erosional character, with a strong wetland reduction of about 20%. This observation is enhanced by the underestimation that occurs in this case, due to the fact that the 1987 tide level was slightly lower than in the other two cases;

- the second period, from 1987 to 1993, showed a positive accretion of wetland extent, with an almost complete recovery of the global loss that occurred during the first period. In this case too, the tidal differences strengthen the accretion observed.

- the overall difference between the extreme dates of the decade showed a modest reduction in the wetland extension.

The entire data-sets analyzed describe the decade as two distinct periods initially characterized by a strong erosive processes, subsequently followed by almost similarly intense accretion activity. The final result coincides with a slight reduction of wetlands, with a global loss gradient of 0.102 km^2/yr, but the change observed in this case (–0.923 km ^{2}) is so small that it lies within the 'error bounds' of the MLH/LMM analysis.

Conclusions and perspectives

The research described here outlines the potential of remote sensing satellite observations to monitor the changes in wetland extension in the estuarine environment.

Multi-temporal satellite imagery, such as Landsat Thematic Mapper data, coupled to an appropriate analysis procedure, allowed us to obtain accurate and an up-to-date information on landscape patterns in order to have a complementary insight into the present trend of the erosion/sedimentation processes in the Venice lagoon,

Table 8. Final land-cover mapping from classification (MLH + LMM) of Landsat TM data for the study area during the observed time period.

Date	Tidal stage (cm)	Wetland areas # Pixels	(km^2)	(%)	Water surface # Pixels	(km^2)	(%)
03 Aug 84	7.83	15507	13.956	41.35	21999	19.799	58.65
08 May 87	4.70	12459	11.213	33.22	25047	22.542	66.78
24 May 93	7.88	14482	13.033	38.61	23024	20.721	61.39

Table 9. Temporal changes in wetland extension obtained from satellite data at intermediate periods between 1984 and 1993. The figures express the absolute and percentage values and the rate of change as km^2 per year.

Time period	Tidal stage difference (cm)	Wetland extent variations (km^2)	(%)	(km^2/yr)	Tidal effects on changes
1984 - 1987	- 3.13	–2.74	–19.63	–0.913	Slight underestimate
1987 - 1993	+ 3.18	+1.82	+16.23	+0.303	Slight underestimate
1984-1993	+ 0.05	–0.923	–6.61	–0.102	Unaffected estimate

although within a limited study area measuring 34 km^2.

Naturally, the influence of tidal stages plays an important role, meaning that compensation of their effects is required. Access to satellite data is a real possibility and not one that is linked to tidal heights. In this paper the results are relative to a specific situation defined by the tide level at 7.80 cm a.m.s.l. Additional investigations will need to be conducted a) in order to identify the magnitude of tidal effects on the ability to detect wetland changes from satellite observations and b) to predict the impact of various sea level rise scenarios on the delicate lagoon environment. This will be achieved with the support of a dedicated GIS and suitable quantitative modeling.

Conventional approaches which are dominant in remote sensing context refer to classifiers producing one class per pixel. The successive application of the maximum likelihood classifier (MLH) and linear mixture model (LMM) techniques allowed estimation of the proportions within each unclassified pixel, improving mapping accuracy. Thus, the adopted strategy proved to be essential for a correct image classification which is the necessary input for reliable assessments on temporal land-cover changes.

The results obtained from the digital analysis of three Landsat Thematic Mapper scenes during the period between 1984 and 1993 showed that the water surface had increased slightly and that consequently, the wetlands had been reduced by about 1 km^2. Moreover, validation through use of independent high resolution data proved that satellite image analysis underestimates the water extension, further supporting the decrease in wetland area.

This confirms that in the Venice lagoon, in accordance with the fact that most of the world's wetlands are deteriorating and decreasing in area, the predominant processes have also been erosive, although at a much lower rate than that observed during the preceding decades for the entire Venice lagoon.

In conclusion, satellite remote sensing can actually 'fill the gap' in terms of the information required for studying the short-term geomorphological changes that typically occur in coastal environments. It can also be used to conduct repetitive surveillance, which would otherwise be almost impossible to achieve with traditional surveys.

Acknowledgments. The authors acknowledge the support by G. Cecconi and V. Macaluso of the Consorzio Venezia Nuova (Venice). They would also like to thank the personnel of CNR-ISDGM (Venice) for all their technical assistance, particularly C. Ramasco and S. Vianello for the ground spectro-radiometric measurements, and A. Tomasin for the computation of tidal heights. Particular thanks are also addressed to the 'Regione del Veneto' for authorizing consultation of aerial photographs. This research was sponsored by the National Research Council of Italy (CNR), 'Sistema Lagunare Veneziano' Project.

References

Anon. 1987. *From pattern to process: the strategy of the Earth Observing System.* EOS Science Steering Committee Report, Vol II. NASA, Washington DC pp. 140.

Anon. 1989. REA-Riequilibrio e Ambiente. *Progetto preliminare di massima delle opere alle bocche*, Vol. I-II, parts 1-2. Consorzio Venezia Nuova, Ministero per i Lavori Pubblici, Magistrato alle Acque di Venezia.

Anon. 1992. *Progetto generale di massima degli interventi morfologici in laguna.* Consorzio Venezia Nuova, Ministero per i Lavori Pubblici, Magistrato alle Acque di Venezia.

Adami, A., Caielli, A., Cecconi, G. & Cianfruglia, A. 1992. Rilievi batimetrici svolti recentemente nella laguna di Venezia. *Proc. 23° Idraulica e Costruzioni Idrauliche*, Firenze, pp. D63-D74.

Adams, J.B., Smith, M.O. & Johnson, P.E. 1986. Spectral mixture modeling: a new analysis of rock and soil types at the Viking Lander 1 site. *J. Geophys. Res.* 91/B8: 8098-8112.

Alberotanza, L. & Lechi, G.M. 1978. Frequency analysis of aerial thermal surveys on shallow water: a methodology to describe the geometric distribution of bottom morphology. *Proc. Int. Symp. on Remote Sensing for Observation and Inventory of Earth Resources and Endagered Environment*, Freiburg, Vol. 2, pp. 1149-1158.

Betetto, E. 1973. *Variazioni della morfologia lagunare desunte dal confronto fra le carte idrografiche della laguna di Venezia del 1931 e del 1971.* Thesis, A.A. 1972-73, Faculty of Science, Università di Padova, Padova.

Carbognin, L., Marabini, F. & Tosi, L. 1995. Land subsidence and degradation of the Venetian littoral. In: Barends, Brouwer & Schroeder (eds.) *Land subsidence*, pp. 391-402. IAHS Publ., The Hague.

Cavazzoni, S. & Crosera, F. 1987. Turbulent structures dependent on tidal currents in the bottom boundary layer of the Venice lagoon. *Il Nuovo Cimento* 10/4: 419-431.

Cisotto, L. 1968. Confronti fra lo stato attuale della laguna di Venezia e quello risultante da una carta del 1534 e da altri documenti relativi alla vecchia laguna rinascimentale. *Boll. Mus. Civ. Stor. Nat. Venezia* 18: 69-89.

Clark, J.A. & Primus, J.A. 1990. Sea-level changes resulting from future retreat of ice sheeets: an effect of CO_2 warming of the climate. In: Toley, M.J. & Shennan, I. (eds.) *Sea-level changes*, pp. 356-370. Basil Blackwell Inc., Oxford.

Congalton, R.G. 1991. A review of assessing the accuracy of classifications of remotely sensed data. *Remote Sens. Environ.* 37: 35-46.

Fitzpatrick-Lins, K. 1981. Comparison of sampling procedures and data analysis for land-use and land-cover map. *Photogram. Eng. Remote Sen.* 47: 343-351.

Gatto, P. & Carbognin, L. 1981. The lagoon of Venice. Natural environment trend and man-induced modification. *Hydrol. Sci. Bull.* 26/4: 379-391.

Goldmann, A., Rabagliati, R. & Sguazzero, P. 1975. Propagazione della marea nella Laguna di Venezia: Analisi dei dati rilevati dalla rete mareografica lagunare negli anni 1972-73. *Riv. Ital. Geofis.* 2/2: 119-131.

Gross, M.F., Hardisky, M.A., Klemas, V. & Wolf, P.L. 1987. Quantification of biomass of the marsh grass *Spartina alterniflora* Loisel using Landsat Thematic Mapper imagery. *Photogram. Eng. Remote Sens.* 53: 1577-1583.

Haddad, K.D. & Ekberg, D.R. 1989. *Potential of Landsat TM imagery for assessing the national status and trends of coastal wetlands.* Proc. 5th Symp. on Coastal & Ocean Management, pp. 5192-5201. American Soc. Civil Eng, New York, NY.

Hardin, P.J. 1994. Parametric and nearest-neighbor methods for hybrid classification: a comparison of pixel assignment accuracy. *Photogramm. Eng. Remote Sensing* 60: 1439-1448.

Holben, B.N. & Shimabukuro, Y.E. 1993. Linear mixing model applied to coarse resolution data from multispectral satellite sensors. *Int. J. Remote Sensing* 14/11: 2231-2240.

Hurcom, S.J., Taberner, M. & Harrison, A.R. 1993. *Mixture modelling of semi-arid vegetation using AVIRIS and SIRIS data.* Proc. 25th ERIM Int. Symp., 4-8 April 1993, Vol. 1, pp. 123-134.

Jensen, J.R., Cowen, D.J., Althausen, J.D., Narumalani, S. & Weatherbee, O. 1993a. An evaluation of the Coast Watch change detection protocol in South Carolina. *Photogramm. Eng. Remote Sens.* 59: 1039-1046.

Jensen, J.R., Cowen, D.J., Althausen, J.D., Narumalani, S. & Weatherbee, O. 1993b. The detection and prediction of sea level changes on coastal wetlands using satellite imagery and a geographic information system. *Geocarto Int.* 4: 87-98.

Markham, B.L. & Barker, J.L. 1985. Spectral characterization of the LANDSAT Thematic Mapper sensors. *Int. J. Remote Sensing* 6 (5): 697-716.

Nilsson, A. 1992. *Greenhouse Earth*. John Wiley & Sons, Chichester.

Richards, J.A. 1986. *Remote sensing digital image analysis: an introduction.* Springer Verlag, Berlin.

Rusconi, A. 1987. *Variazione delle superfici componenti il bacino lagunare.* Pubblicazione n. 160, Ufficio Idrografico Magistrato alle Acque, Venezia.

Santangelo, R., Tomasin, A., Ghermandi, G., Pugnaghi, S. & Canestrelli, P. 1982. *High water in Venice.* Proc. Conf. "Polders of the world", Lelystad.

Shimabukuro, Y.E. & Smith, J.A. 1991. *The least-squares mixing models to generate fraction images derived from remote sensing multispectral data.* IEEE Trans. Geosci. Remote Sens. GE-29/1: 16-20.

Swain, P.H. & Davis, S.M. 1978. *Remote sensing: the quantitative approach*. McGraw Hill, New York, NY.

Terayama, Y., Ueda, Y., Arai, K. & Matsumoto, M. 1992. *A comparative study on the methods for estimation of mixing ratio within a pixel.* Proc. 17th ISPRS Symp., Vol. 29-B7, pp. 986-989. Washington, DC.

Thomas, R.H. 1986. Future sea level rise and its early detection by satellite remote sensing. In: Titus, J.G. (ed.) *Effects of changing stratospheric ozone and global climate*, pp. 19-36. US Environ Protection Agency, Washington, DC.

Verger, F. & Demathieu, P. 1973. Etude diachronique des surfaces d'eau et des surfaces mouillées sur deux images ERTS 1. *Photo-Interprétation*, 5: 1-7.

Wigley, T.M.L. & Raper, S.C.B. 1993. Future changes in global mean temperature and sea level. In: Warrick, R.A., Barrow, E.M. & Wigley, T.M.L. (eds.) *Climate and sea level changes: observations, projections and implications*, pp. 111-133. Cambridge University Press, Cambridge.

Zilioli, E., Brivio, P.A., Arrigazzi, M. & Lechi, G.M. 1994. Sub-pixel estimation of the Venice lagoon wetlands using Thematic Mapper data. In: Chavez, P.S. Jr., Marino, C.M. & Schowengerdt, R.A. (eds.) *Recent Advances in Remote Sensing and Hyperspectral Remote Sensing*, pp.101-108. SPIE 2318, Bellingham, Washington, DC.

Received 11 May 1995;
Revision received 18 February 1996;
Accepted 27 March 1996;
Final version received 22 May 1996.